High-pressure synchrotron-diffraction study of the superconducting spin-ladder compounds $(Sr, M)_{14}Cu_{24}O_{41}$ (M = Ca, Ba, Nd)

Stéphanie Pachot and Pierre Bordet
Laboratoire de Cristallographie CNRS, Boîte Postale 166, 38042 Grenoble Cedex 9, France

Robert J. Cava
Department of Chemistry and Materials Institute, Princeton University, Princeton, New Jersey 08540

Catherine Chaillout and Céline Darie
Laboratoire de Cristallographie CNRS, Boîte Postale 166, 38042 Grenoble Cedex 9, France

Michael Hanfland
European Synchrotron Radiation Facility, Boîte Postale 220, 38043 Grenoble, France

Massimo Marezio
MASPEC-CNR, via Chiavari 18/A, 43100 Parma, Italy

Hidenori Takagi
Institute for Solid State Physics, University of Tokyo, Roppongi Minato-ku, Tokyo 106, Japan
(Received 19 October 1998)

The evolution of the cell parameters as a function of pressure of five samples of the spin-ladder compounds $(Sr, M)_{14}Cu_{24}O_{41}$, with M = Ca, Ba, Nd has been investigated up to ≈10 GPa by high-pressure synchrotron x-ray diffraction on the ID9 beam line of the ESRF. A large anisotropy of compressibility is observed, with a very strong compression along the *b* axis, corresponding to the stacking direction of the ladder and chain layers. A striking lattice anomaly is detected in the 5–8 GPa range, depending on composition. It consists of an abrupt increase of the *a* parameter value, a measure of the in-plane separation between ladders, with increasing pressure. This anomaly could play a role in the disappearance of superconductivity above ≈6 GPa in this system. [S0163-1829(99)00818-8]

INTRODUCTION

Following the discovery of high-T_c superconducting cuprates, the theoretical investigation of the magnetic and transport properties in low-dimensional copper oxide systems has become increasingly active. Recently, the so-called ''spin-ladder'' systems have drawn much of the attention, due to their predicted striking properties. Spin ladders are quasi-one-dimensional objects resulting from the coupling by corner sharing of parallel and infinite chains of CuO_4 squares (the ladder legs).

The peculiar physical properties of spin ladders originate from the competition between magnetic interactions along the legs and rungs of the spin-1/2 Cu^{2+} cations. The properties depend on the relative strengths of these interactions, as well as on the parity of the number of ladder legs. Dagotto and Rice[1] predicted the existence of a spin gap, when the antiferromagnetic coupling along rungs is present, and Rice *et al.*[2] showed that this property would only exist for even leg ladders. They also predicted the appearance of superconductivity when holes are introduced in this system. The existence of a spin gap was experimentally verified by Azuma *et al.*,[3] in the homologous series of general formula $Sr_nCu_{n+1}O_{2n+1}$. However, these authors were unable to chemically modify these materials in order to induce hole doping, and did not succeed in finding superconductivity at low temperature.

Superconductivity was detected in a compound containing spin ladders by Uehara *et al.*,[4] who measured the resistivity as a function of pressure and temperature in the $(Sr_{14-x},Ca_x)Cu_{24}O_{41}$ compounds. These authors reported the appearance of a superconducting transition in the 3–5 GPa range, with a maximum transition temperature of about 12 K, in samples with a large calcium concentration ($x = 13.6$). This discovery was the starting point of a large, still continuing, experimental effort to investigate the physical properties of this system and understand the nature of its normal and superconducting states.

The structure of $(Sr_{14-x},Ca_x)Cu_{24}O_{41}$ (Fig. 1) can be described as the alternate stacking of layers having the two-leg-ladder arrangement and Cu_2O_3 composition, and layers made of isolated chains of edge-sharing CuO_4 squares, separated by planes containing the alkaline earth cations. The ladder planes are formed by the corner-sharing connection of double chains of edge-sharing CuO_4 squares. Within the double chains, the Cu cations are linked through 90° Cu-O-Cu bonds, leading to geometrical spin frustration and weak magnetic coupling. Consequently the ladders may be considered as magnetically quasi-isolated objects. The CuO_4 squares belonging to the chains above and below are oriented at 45° with respect to the CuO_4 squares belonging to the ladders. The incommensurate $\sqrt{2}$ ratio between the Cu-Cu separation in both types of layers resulting from this arrange-

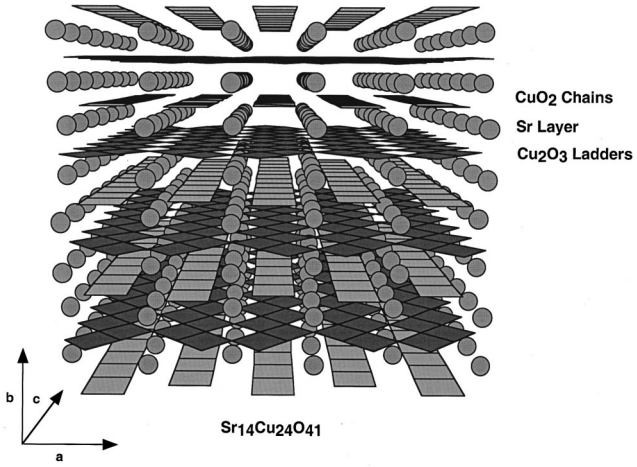

FIG. 1. An idealized view of the $Sr_{14}Cu_{24}O_{41}$-type structure.

ment, leads to a composite type of structure, which in a first approximation can be described by using two orthorhombic unit cells with parameters: $a_l \approx 11.4$ Å, $b_l \approx 13.0$ Å, and $c_l \approx 3.92$ Å for the $Sr(Cu_2O_3)Sr$ ladder-containing slabs, and $a_c = a_l$, $b_c = b_l$, and $c_c \approx 2.75$ Å $\approx 7/10 \times c_l$ for the chain layers. The *a* direction is in the plane of, and perpendicular to the chains and ladders; the *b* direction is perpendicular to the stacking, and the *c* direction is along the chains and ladders. However, this schematic description of the structure may be oversimplified, and thorough crystallographic studies[5,6] pointed out the presence of buckling in both ladder and chain layers, and of interlayer Cu-O bonds which may play an important role in the doping mechanism.

Optical measurements have shown[7] that the intrinsic hole doping due to the 2.25+ average copper valence is gradually transferred from the chains to the ladders with increasing calcium concentration. Since this substitution is isovalent, the doping modification is induced by altering the average size of the (Sr, Ca) mixed site, which leads to changes of the Cu-O bond lengths in both chains and ladders. Due to the smaller ionic size of Ca cations, the effect of Ca substituting for Sr can be viewed as a chemical pressure effect. Since the superconducting properties of the $(Sr_{14-x},Ca_x)Cu_{24}O_{41}$ compound appear only at high pressure and for specific calcium concentrations, it is of the highest relevance to investigate the evolution of the structure with pressure and composition. Therefore, we have carried out a high-pressure synchrotron-diffraction experiment at room temperature in the 0–10 GPa range for a set of $(Sr_{14-x},M_x)Cu_{24}O_{41}$ samples with $M = Ca$, Ba, Nd, and x between 0 and 13.6 in order to investigate the combined effects of applied pressure, and modification of the average ionic size and/or valence of the (Sr, *M*) mixed site.

EXPERIMENTAL

Five different samples of $(Sr_{14-x},M_x)Cu_{24}O_{41}$ general formula were used for this experiment, hereafter denoted as: Sr14: $x = 0$; Sr8Ca6: $M = Ca$, $x = 6$; SrCa13: $M = Ca$, $x = 13.6$ (superconducting composition); Sr10Ba4: $M = Ba$, $x = 4$; Sr8Nd6: $M = Nd$, $x = 6$. The first four samples were used to investigate the effect of pressure as a function of the average size of the mixed site, while the data comparison between Sr8Ca6 and Sr8Nd6 allows us to compare the effect of changing only the average valence of this site (Nd^{3+} and Ca^{2+} cations have very close ionic sizes). They were previously characterized for cationic stoichiometry and phase purity by energy-dispersive spectroscopy (EDS) analysis and laboratory powder x-ray diffraction. During the high-pressure experiment, the Sr14 sample showed signs of partial decomposition, with the appearance of weak peaks from parasitic phases and an anomalously high value of the c_l cell parameter (3.975 Å instead of 3.957 Å as determined by laboratory x-ray diffraction).

The high-pressure synchrotron-diffraction experiment was carried out at the ID9 beamline of the European Synchrotron Radiation Facility (ESRF) using angle-dispersive powder diffraction with image plates as detectors. Samples were loaded into a 130 μm diameter and 35 μm high gasket hole of a membrane diamond-anvil cell. Pressures were measured using the ruby-fluorescence method.[8] Silicone oil was used as pressure transmitting medium. Though it is known to be a rather poorly hydrostatic medium above 6 GPa, it was chosen because of its inert character with respect to the samples. In order to check the effect of pressure gradients induced by this medium at higher pressures, two additional experiments

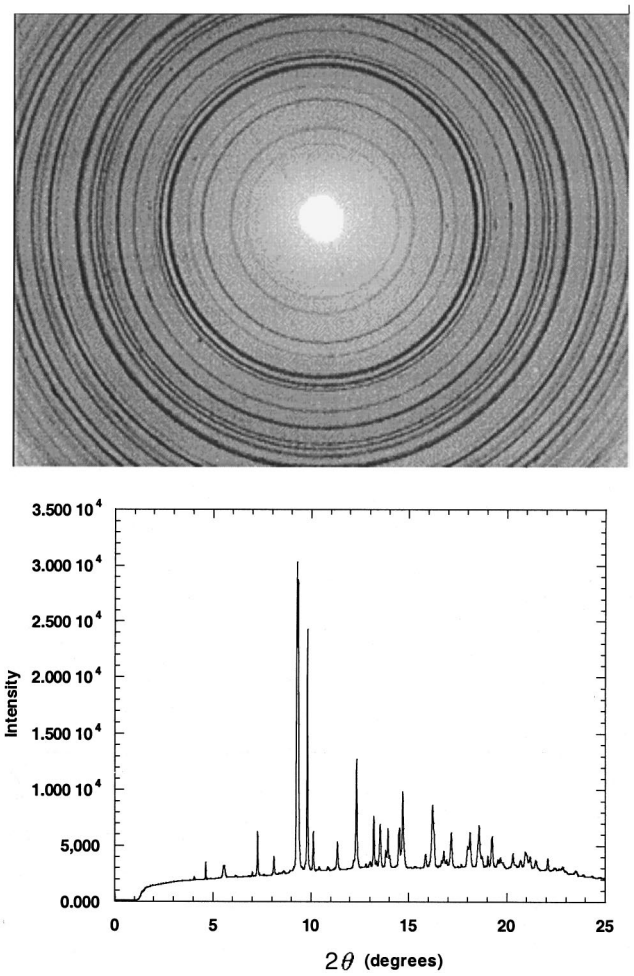

FIG. 2. Diffraction spectrum obtained at 0.1 GPa for the $(Sr_8,Nd_6)Cu_{24}O_{41}$ sample. (a) Partial raw image plate data showing the diffraction rings from the sample. (b) Corresponding $I(2\theta)$ spectrum after image corrections and azimuthal averaging as described in text.

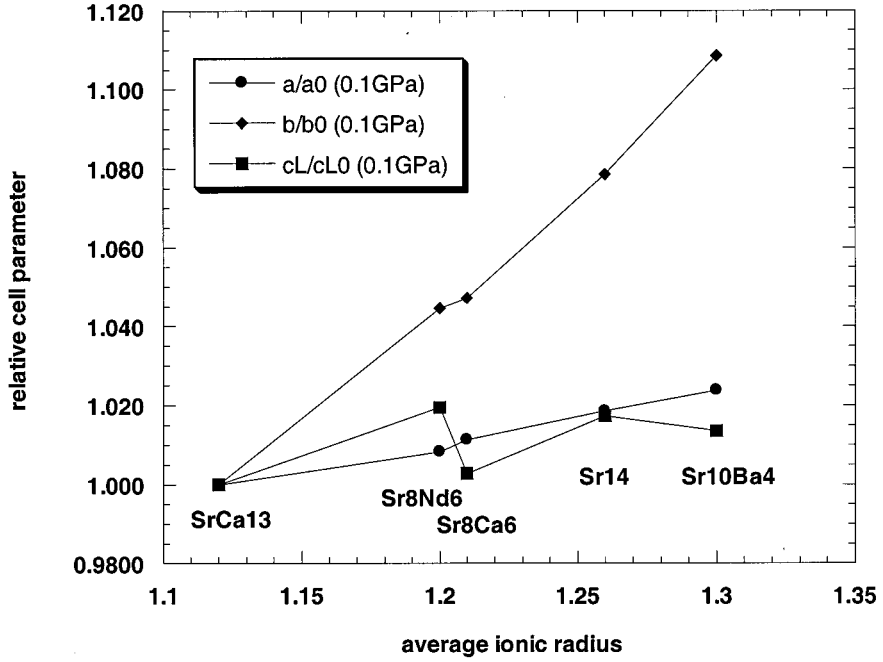

FIG. 3. Relative evolution of the cell parameters as a function of average ionic radius of the mixed cation site (Å) at ≈0.1 GPa. The average radii have been computed from tabulated data (Ref. 12), using the cation stoichiometries obtained by EDS analysis. The normalization has been made with respect to the $(Sr_{0.4},Ca_{13.6})Cu_{24}O_{41}$ compound.

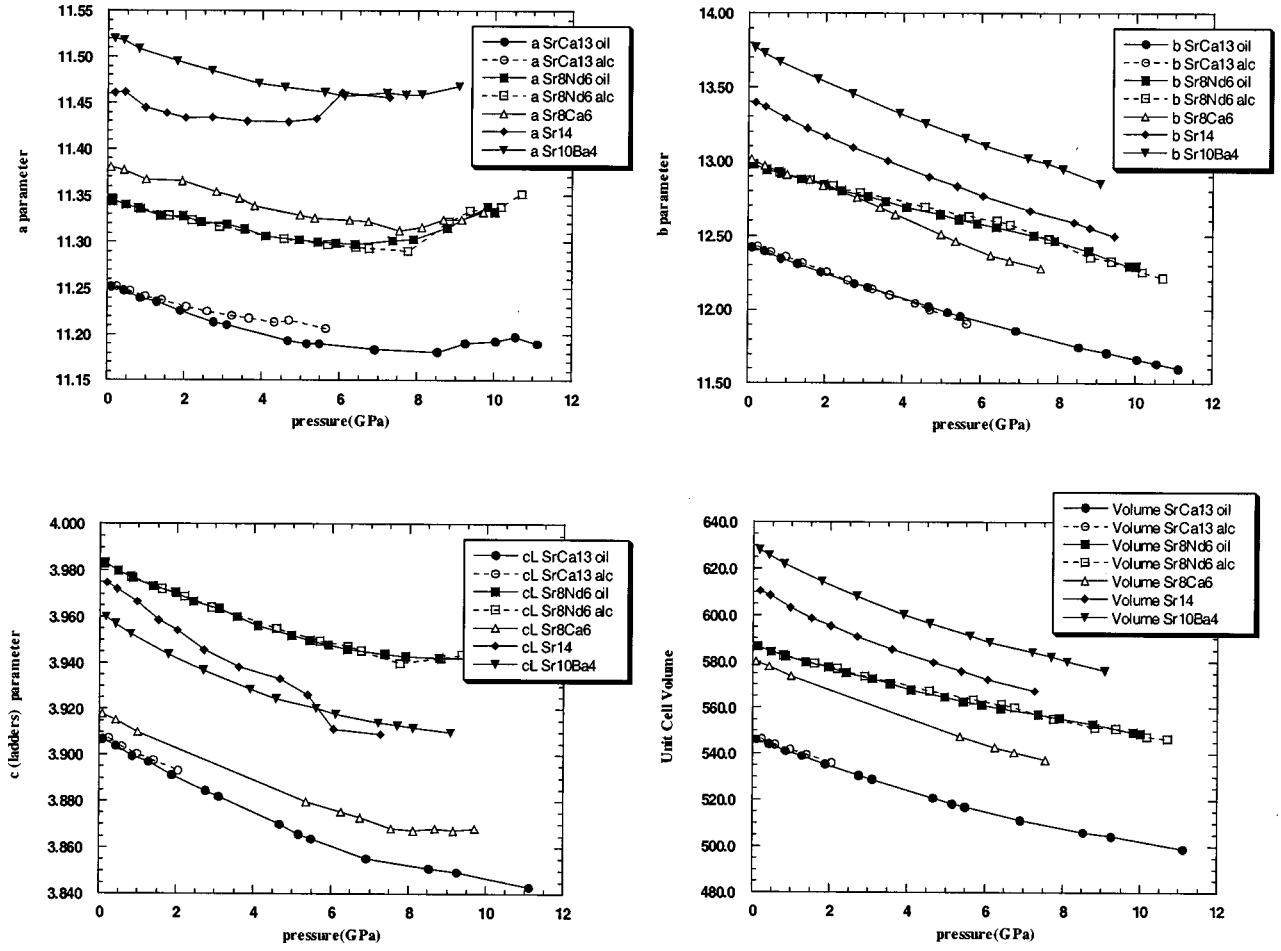

FIG. 4. Evolution of the cell parameters (Å) and volume ($Å^3$) up to ≈10 GPa for the five samples investigated. The ''oil'' and ''alc'' terms refer to silicone oil or methanol/ethanol mixture being used as pressure transmitting medium, respectively.

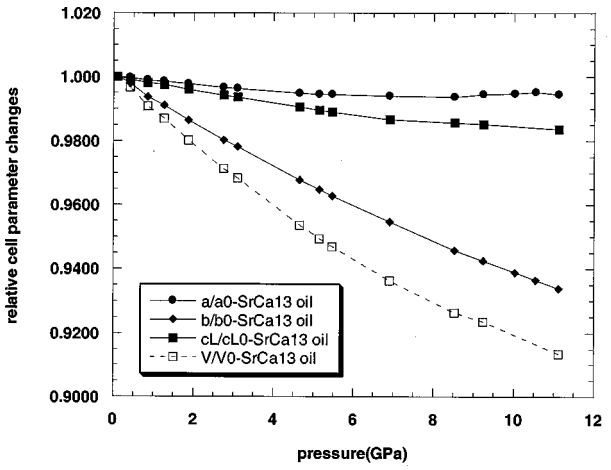

FIG. 5. Relative evolution of the cell parameters and volume as a function of pressure for the $(Sr_{0.4},Ca_{13.6})Cu_{24}O_{41}$ compound, using silicone oil as pressure transmitting medium.

were carried out on samples Sr8Nd6 and SrCa13, by using a 4:1 methanol/ethanol mixture, known to remain a better pressure transmitter to 10 GPa. The results obtained were similar for the Sr8Nd6 sample, but the SrCa13 sample started to decompose above 3 GPa in the methanol/ethanol mixture, leading to the appearance of calcium and copper containing phases. The difference in behavior between these two samples is probably related to their different chemical compositions. Calcium containing phases have in general a poorer chemical stability, especially with respect to water, which may be contained as impurity in the methanol/ethanol mixture. Nevertheless, the similar results obtained for the Sr8Nd6 sample with both transmitting media indicate that the observed effects described below are not due to pressure gradients brought about by silicone oil at high pressures.

The monochromatic beam ($\lambda = 0.458$ Å) was selected by a horizontally focusing asymmetrically cut bent Si(111) Laue monochromator.[9] It was vertically focused by a curved Pt-coated Si mirror. The beam size on the sample was 30 $\times 30\,\mu$m. Diffraction rings from the powder samples were recorded on an A3 size Fuji image plate located at 441 mm from the sample. The plates were scanned on a molecular-dynamics image plate reader, and processed by using the FIT2D software developed at the ESRF.[10] The images [one is shown in Fig. 2(a)] were corrected for spatial distortion effects due to reader imperfections, by applying a transformation deduced from the analysis of a calibrated grid image. Corrections for the image plate tilt with respect to the direct beam were applied by using images from a standard silicon powder, which were periodically measured during the experiment. These images were also used to calibrate the wavelength and the sample to detector distance. After removal of spurious peaks (from the diamonds, rubys, etc . . .) the corrected images were averaged over 360° about the direct beam position, yielding intensity vs 2θ spectra similar to those obtained by classical diffraction techniques [Fig. 2(b)].

Due to the complexity of the structure, we did not attempt to refine any positional parameters using, for example, the Rietveld technique, but concentrated our analysis on the evolution of the cell parameters with pressure. Even for this purpose, the broadening of Bragg reflections and the large number of overlapping of peaks at high pressures prevented in some cases a reliable determination of the positions of a sufficient number of lines in the whole pressure range to perform unbiased refinement of the cell parameters. Therefore, we selected for each sample a set of diffraction lines (generally at low 2θ angles) which were well isolated in the whole pressure range, and obtained their angular positions by least-square refinement using a pseudo-Voigt line-shape function. The cell parameters were obtained by transforming the 2θ positions into d values using the Bragg's law. Note that in most cases, it was not possible to identify isolated peaks from the ''chain'' unit cell, so only the parameters $a_c = a_l$, $b_c = b_l$, and c_l from the ''ladder'' unit cell could be obtained.

RESULTS AND DISCUSSION

Evolution of the cell parameters with composition at room pressure

The relative evolution of the cell parameters at $P \approx 0.1$ GPa is shown in Fig. 3, as a function of the average ionic radius of the mixed site. The normalization was made with respect to the SrCa13 sample. The cell parameter increase with increasing average ionic radius of the mixed site is strongly anisotropic, with a much larger effect in the b

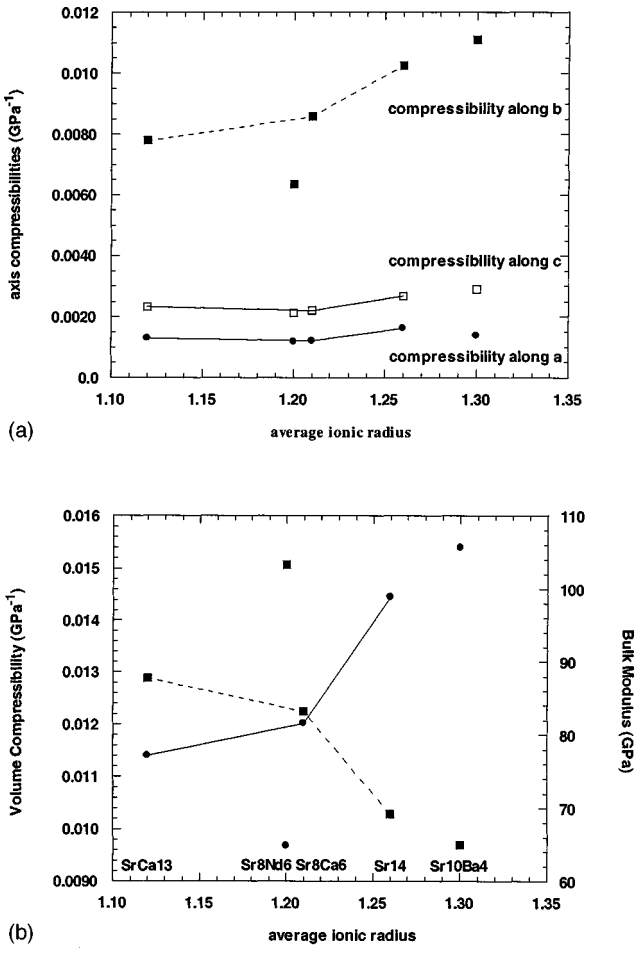

FIG. 6. Axis compressibilities (a), volume compressibility and bulk modulus (b) for the five samples investigated, as a function of average ionic radius of the mixed cation site (Å).

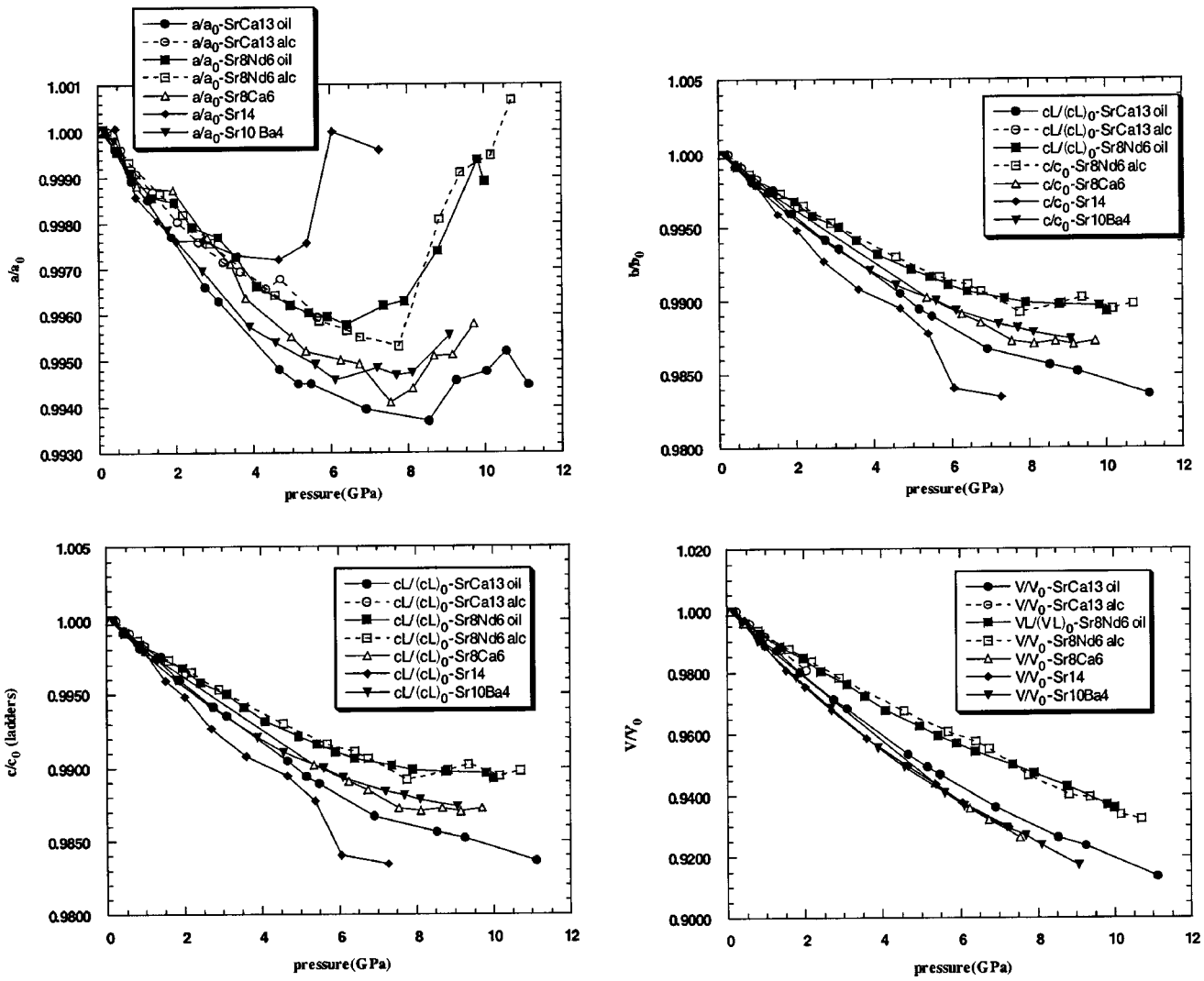

FIG. 7. Relative evolution of the cell parameters and volume as a function of pressure for the five samples investigated. The ''oil'' and ''alc'' terms refer to silicone oil or methanol/ethanol mixture being used as pressure transmitting medium, respectively.

direction, and the smallest effect along *c*. This is most probably due to the weakness of ionic bonds along the stacking direction with respect to the strong in-plane Cu-O bonds inside the ladder and chain layers. A similar anisotropy is to be expected for the effect of pressure. It is interesting to point out that the *a* and *b* cell parameters of the Sr8Nd6 sample follow the regular evolution due to size effects, while the *c* parameter value is markedly higher. This indicates that the charge effect brought about by the replacement of Ca^{2+} by Nd^{3+} cations leads to modifications of the Cu-O bonding scheme mainly along the chain and ladder directions.

Evolution of the cell parameters as a function of composition and pressure

The evolution of the cell parameters and volume as a function of pressure is shown for each sample in Fig. 4. Only the points where the cell parameter values could be determined unambiguously by the procedure described above have been reported. At first glance, all samples, except Sr8Nd6, exhibit a similar behavior, with roughly parallel decreases of the cell parameters and volume with increasing applied pressure. As an example, the relative evolutions of cell parameters and volume are shown in Fig. 5 for the SrCa13 sample. It can be seen that the compressibility is strongly anisotropic, with a somewhat easy compression along the *b* axis direction, and hard along *a*.

The axis compressibilities are reported in Fig. 6(a), while the volume compressibility and bulk modulus are shown in Fig. 6(b). The compressibility is the smallest in the *a* axis direction, with values ranging from 1.3 to 1.6 $\times 10^{-3}\,\mathrm{GPa}^{-1}$. The compressibility along *c* is about twice as large as that along *a*, with values ranging from 2.1 to 2.9 $\times 10^{-3}\,\mathrm{GPa}^{-1}$. For both directions, the compressibility increases slightly with increasing average radius of the mixed site, and the obtained values are close to those reported for the in-plane compressibilities of superconducting cuprates.[11] The *b*-axis compressibility is much larger than the in-plane ones, with values ranging between 6.3 and 11 $\times 10^{-3}\,\mathrm{GPa}^{-1}$. These values are twice as large as the largest *c*-axis compressibilities reported for the superconducting cuprates. Moreover, the *b*-axis compressibility markedly increases with increasing average ionic radius of the mixed cation site. This could indicate an increase of interlayer interactions when the size of the mixed site is decreased, i.e.,

when the ladder and chain layers come closer to each other. The *b*-axis compressibility of the Sr8Nd6 sample is anomalously low with respect to the values obtained for the other samples, as can be seen from the plot of Fig. 4(b). Thus, the charge effect brought about by the replacement of Ca^{2+} by Nd^{3+} does not affect the *b* parameter value (Fig. 3), but has a strong impact on the *b*-axis compressibility. The origin of this effect could be the strengthening of chemical bonds in the stacking direction related to the increased average valence of the mixed site.

In Fig. 7, we present the relative evolution of the cell parameters and volume as a function of pressure. The most striking feature observed, is the presence of a lattice anomaly consisting in a strong increase of the *a* cell parameter above 6–8 GPa, depending on sample composition. The reproducibility of this anomaly, particularly for the two experiments carried out with the Sr8Nd6 sample, using silicone oil and methanol/ethanol mixture as pressure transmitting media (full and empty squares in Fig. 7, respectively), demonstrate that it is not due to an experimental artifact. The softer transition observed for Sr8Nd6 using silicone oil is probably related to the presence of larger pressure gradients. It is worth noting that, for this sample, the *a* parameter value is larger at 11 GPa than at room pressure. In some cases, the *a* parameter seems to start decreasing again at higher pressures. However, we were not able during this experiment to reach pressures high enough to confirm this effect. The pressure value at which the anomaly takes place seems to increase with increasing Ca content, going from $\approx$5 GPa for Sr14, to $\approx$7.5 GPa for Sr8Ca6, and to $\approx$8.5 GPa for SrCa13. For Sr10Ba4 and Sr8Nd6, the anomaly appears at $\approx$7.5 GPa. For the Sr8Nd6 sample, above the *a*-axis anomaly pressure value, the *c* parameter seems to become stable, and the *b*-axis compressibility starts to increase again. The former effect seems to exist also for the other samples, even though less pronounced. The diffraction spectra recorded at pressures above the lattice anomaly do not present noticeable differences, such as peak splitting or superlattice reflections, from those recorded below, indicating that no major structural rearrangement is occurring at the transition.

Although the present data do not allow us to draw definitive conclusions about the nature of this lattice anomaly, a possible origin could be the abrupt decrease of the ladder and chain layer buckling induced by the applied pressure. Such an effect could indeed lead to an increase or stabilization of the in-plane cell parameters *a* and *c*, and allow the restoration of the compressibility in the *b*-axis stacking direction. The effect of applied pressure and lattice anomaly on the physical and superconducting properties of the $(Sr_{14-x},M_x)Cu_{24}O_{41}$ compounds may be discussed on the basis of the present results and already reported structural and physical measurements.[5–7] The main effect of the substitution of Ca for Sr and of applied pressure is a strong decrease of the *b* cell parameter, which corresponds to an increased coupling between the ladder and chain layers, and to a charge transfer from the chains to the ladders. The similarity between the substitution and pressure effects on the cell parameter indicates that the cation substitution acts as an internal chemical pressure. However, the substitution effect alone is not sufficient to induce superconductivity at low temperature, and an additional external pressure has to be applied, with appearance of the superconducting state at $\approx$3 GPa for the $(Sr_{0.4},Ca_{13.6})Cu_{24}O_{41}$ compound, which corresponds to a cell parameter $b \approx 12.15$ Å. The disappearance of superconductivity above $\approx$6 GPa might be related to the lattice anomaly, even though it seems to appear at higher pressures ($\approx$8.5 GPa for the SrCa13 sample) at room temperature. Low-temperature and high-pressure diffraction experiments are needed to confirm this model.

[1] E. Dagotto and T. M. Rice, Science **271**, 618 (1995).

[2] T. M. Rice, S. Gopalan, and M. Sigrist, Europhys. Lett. **23**, 445 (1993).

[3] M. Azuma, Z. Hiroi, M. Takano, K. Ishida, and Y. Kitaoka, Phys. Rev. Lett. **73**, 3463 (1994).

[4] M. Uehara, T. Nagata, J. Akimitsu, H. Takahashi, N. Mori, and K. Kinoshita, J. Phys. Soc. Jpn. **65**, 2764 (1996).

[5] A. Frost-Jensen, B. B. Iversen, V. Petricek, T. M. Schultz, and Y. Gao, Acta Crystallogr., Sect. B: Struct. Sci. **53**, 113 (1997).

[6] T. Ohta, F. Izumi, M. Onoda, M. Isobe, E. Takayama-Muromachi, and A. W. Hewat, J. Phys. Soc. Jpn. **66**, 3107 (1997).

[7] T. Osafune, N. Motoyama, H. Eisaki, and S. Uchida, Phys. Rev. Lett. **78**, 1980 (1997).

[8] H. K. Mao, J. Xu, and P. M. Bell, J. Geophys. Res. **91**, 4673 (1986).

[9] C. Schulze, U. Lienert, M. Hanfland, M. Lorenzen, and F. Zontone, J. Synchr. Radiat. (to be published).

[10] A. P. Hammersley, S. O. Svensson, M. Hanfland, A. N. Fitch, and D. Häusermann, High Press. Res. **14**, 235 (1996).

[11] H. Takahashi and N. Mori, in *Studies of High Temperature Superconductors*, edited by A. Narlikar (Nova Science, Commack, NY, 1996), Vol. 16, p. 1.

[12] R. D. Shannon, Acta Crystallogr., Sect. A: Cryst. Phys., Diffr., Theor. Gen. Crystallogr. **32**, 751 (1976).